TRACKING DOWN PENGUINS AT THE POLES

J.-M. GERARD,[1] C. SMITH,[2] S. TRINE [3,a]

[1] *Institut de Physique Théorique, Université catholique de Louvain, Chemin du Cyclotron 2, B-1348 Louvain-la-Neuve, Belgium*

[2] *Institut für Theoretische Physik, Universität Bern, CH-3012 Bern, Switzerland*

[3] *Institut für Theoretische Teilchenphysik, Universität Karlsruhe, D-76128 Karlsruhe, Germany*

QCD penguins are responsible for about 2/3 of the $\Delta I = 1/2$ rule in $K \to \pi\pi$ decays, as inferred from a combined analysis of $K \to \pi\pi$ and $K_L \to \gamma\gamma$. Further tests based on the decays $K_S \to \pi^0\gamma\gamma$ and $K^+ \to \pi^+\gamma\gamma$ are proposed. New insights into the treatment of π^0, η, η' pole amplitudes are also reported.

1 Introduction

Recently, a systematic analysis of η_0 pole contributions to radiative K decays was performed in the context of large N_c ChPT, in order to better understand the role of gluonic penguin operators in $K \to \pi\pi$ transitions[1]. In this note, we emphasize some aspects of this study, in view of the forthcoming new experimental information on $K^+ \to \pi^+\gamma\gamma$ by the NA48 Collaboration[2]. A number of issues, like the correspondence between the $SU(3)$ and $U(3)$ chiral expansions, the impact of our analysis for $K_L \to \gamma\gamma^*$, $K_L \to \pi^0\pi^0\gamma\gamma$ and $K_L \to \pi^+\pi^-\gamma$, or the fate of the weak mass operator, are left to the original paper.

2 General framework

The effective weak Hamiltonian relevant to describe (CP-conserving) hadronic K decays reads:

$$\mathcal{H}_{eff}^{\Delta S=1}(\mu < m_c) \simeq \frac{G_F}{\sqrt{2}} V_{ud}V_{us}^* \left[z_1(\mu)\, Q_1(\mu) + z_2(\mu)\, Q_2(\mu) + z_6(\mu)\, Q_6(\mu)\right], \tag{1}$$

[a] Speaker

with the familiar current-current operators

$$Q_1 = 4\,(\bar{s}_L\gamma_\alpha d_L)\,(\bar{u}_L\gamma^\alpha u_L)\,, \quad Q_2 = 4\,(\bar{s}_L\gamma_\alpha u_L)\,(\bar{u}_L\gamma^\alpha d_L)\,, \tag{2}$$

and the density-density dominant penguin operator

$$Q_6 = -8\,(\bar{s}_L q_R)\,(\bar{q}_R d_L)\,. \tag{3}$$

In our notations, $q_L^R \equiv \frac{1}{2}(1 \pm \gamma_5)q$ and the light flavours $q = u, d, s$ are summed over. The effective coupling constants $z_i\,(\mu)$ contain QCD effects above the renormalization scale μ, kept high enough to allow the use of perturbation theory. In order to investigate the effects of long-distance strong interactions, we will make use of ChPT (Chiral Perturbation Theory) techniques.

ChPT relies on the $SU(3)_L \times SU(3)_R$ symmetry of the QCD Lagrangian in the massless limit to build a dual representation, in terms of meson fields. If one formally considers the number of QCD colours N_c as large, $SU(3)$ can be extended to $U(3)$ and the spontaneous symmetry breaking $U(3)_L \times U(3)_R \rightarrow U(3)_V$ gives rise to a nonet Π of pseudoscalar Goldstone bosons, which are written $U \equiv \exp(i\sqrt{2}\Pi/F)$ in the standard parametrization. This extension to $U(3)$ will prove crucial afterwards. The corresponding leading nonlinear Lagrangian reads

$$\mathcal{L}_S^{(p^2,\infty)+(p^0,1/N_c)} = \frac{F^2}{4}\langle\partial_\mu U \partial^\mu U^\dagger\rangle + \frac{F^2}{4}\langle\chi U^\dagger + U\chi^\dagger\rangle + \frac{F^2}{16N_c} m_0^2 \langle \ln U - \ln U^\dagger\rangle^2 \tag{4}$$

where $\langle\rangle$ denotes a trace over flavours, the external source χ is frozen at $\chi = rM$ with $M = diag(m_u, m_d, m_s)$ to account for meson masses, F is identified with the pion decay constant $F_\pi = 92.4$ MeV at this order and m_0 represents the anomalous part of the η_0 mass. Note that the leading $SU(3)$ chiral Lagrangian is recovered in the limit $m_0 \rightarrow \infty$, when the η_0 decouples.

The meson realization of Eq.(1) can be obtained from the chiral representations of the corresponding quark currents and densities, i.e., preserving the colour and flavour structures:

$$\mathcal{H}_{eff,\mathcal{O}(p^2)}^{\Delta S=1}\,(\mu \sim m_{\pi,K}) \simeq \frac{G_F}{\sqrt{2}} V_{ud} V_{us}^* \left[x_1\hat{Q}_1 + x_2\hat{Q}_2 + x_6\hat{Q}_6\right], \tag{5}$$

with

$$\hat{Q}_1 = 4\,(L_\mu)_{23}\,(L^\mu)_{11}\,, \quad \hat{Q}_2 = 4\,(L_\mu)_{13}\,(L^\mu)_{21}\,, \quad \hat{Q}_6 = 4\,(L_\mu L^\mu)_{23}\,, \tag{6}$$

and the left-handed currents $(L_\mu)^{lk} \equiv i\frac{F^2}{2}\left(\partial_\mu U U^\dagger\right)^{lk}$. The weak coefficients x_i are not fixed by symmetry arguments, and contain both short-distance and long-distance strong interaction effects. The latter are known to be important in explaining the $\Delta I = 1/2$ rule observed in $K \rightarrow \pi\pi$ decays[3]. Still, the genuine mechanism responsible for the $\Delta I = 1/2$ enhancement, i.e., the relative strength of the penguin and current-current operators, has not been completely settled yet. In this work, we propose a phenomenological extraction of the x_i parameters, and thus of the penguin fraction $\mathcal{F}_P = 3x_6/(-x_1 + 2x_2 + 3x_6)$.

To reach this goal, it is clear that one has to go beyond the standard $SU(3)$ ChPT which only contains two independent weak operators (Q_8 and Q_{27}) such that current-current and penguin operators cannot be disentangled. On the other hand, in $U(3)$, the presence of η_0 as a dynamical degree of freedom allows for an extra $\mathcal{O}(p^2)$ weak operator

$$Q_8^s = 4\,(L_\mu)_{23}\,\langle L^\mu\rangle \sim (L_\mu)_{23}\,\partial^\mu\eta_0, \tag{7}$$

which, together with the straightforward extensions of Q_8 and Q_{27} to $U(3)$

$$Q_8 = 4\,(L_\mu L^\mu)_{23}\,, \quad Q_{27} = 4\left[(L_\mu)_{23}\,(L^\mu)_{11} + \tfrac{2}{3}\,(L_\mu)_{13}\,(L^\mu)_{21} - \tfrac{1}{3}\,(L_\mu)_{23}\,\langle L^\mu\rangle\right], \tag{8}$$

permits now to write the effective Hamiltonian in a way equivalent to Eq.(5):

$$\mathcal{H}_{eff,\mathcal{O}(p^2)}^{\Delta S=1}\,(\mu \sim m_{\pi,K}) \simeq G_8 Q_8 + G_{27} Q_{27} + G_8^s Q_8^s. \tag{9}$$

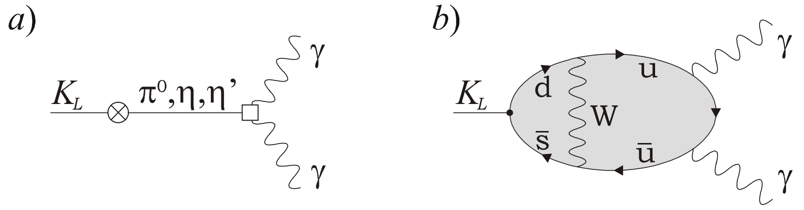

Figure 1: a) Pole diagrams for $K_L \to \gamma\gamma$. b) Dominant long-distance $\bar{u}u$ contribution.

Explicitly, this change of basis reads ($G_W \equiv G_F V_{ud} V_{us}^*/\sqrt{2}$):

$$G_8/G_W = -\tfrac{2}{5}x_1 + \tfrac{3}{5}x_2 + x_6, \quad G_8^s/G_W = \tfrac{3}{5}x_1 - \tfrac{2}{5}x_2, \quad G_{27}/G_W = \tfrac{3}{5}(x_1 + x_2). \tag{10}$$

G_8 and G_{27} are still extracted from $K \to \pi\pi$. The knowledge of G_8^s would thus give access to the x_i parameters, and consequently to $\mathcal{F}_P$. Because of Eq.(7), natural candidates for its extraction are anomaly-driven radiative K decays, that receive a η_0 pole contribution.

3 Penguin fraction in $K \to \pi\pi$ vs η_0 effects in $K_L \to \gamma\gamma$

Due to the well-known pole cancellations at work in $K_L \to \gamma\gamma$, we propose a two-step analysis for this mode:

Step 1: work with the *theoretical* masses m_π, m_η, $m_{\eta'}$, i.e., consistently at a given order in ChPT, in order to identify the vanishing pole contributions (Fig.1a). It turns out that Q_8 does not contribute at $\mathcal{O}(p^4)$, just like in $SU(3)$ ChPT. The leading contribution, of $\mathcal{O}(p^4)$, comes from the $\overline{u}u$ intermediate state generated by $\hat{Q}_1$ (Fig.1b), and is thus proportional to $G_W x_1 = G_8^s + 2G_{27}/3$, i.e., the nonet-symmetry breaking couplings.

Step 2: freeze the π^0, η, η' poles at the *physical* values M_π, M_η, $M_{\eta'}$ to ensure correct analytical properties for the remaining contributions ($\hat{Q}_1$) only. This is done through the following prescription for the η-η' propagator:

$$iP_{phys}\left(q^2\right)^{-1}_{\eta_8\eta_0} = \begin{pmatrix} \cos\theta_P & \sin\theta_P \\ -\sin\theta_P & \cos\theta_P \end{pmatrix} \begin{pmatrix} q^2 - M_\eta^2 & 0 \\ 0 & q^2 - M_{\eta'}^2 \end{pmatrix} \begin{pmatrix} \cos\theta_P & -\sin\theta_P \\ \sin\theta_P & \cos\theta_P \end{pmatrix}, \tag{11}$$

where the parametrisation in terms of one mixing angle is allowed as we work at lowest order in the chiral expansion, cf. Eq.(4). A discussion of two-angle pole formulas may be found in our original paper [1].

The resulting pole amplitude ($c_\theta \equiv \cos\theta_P$, $s_\theta \equiv \sin\theta_P$),

$$\begin{aligned} \mathcal{A}^{\mu\nu}\left(K_L \to \gamma\gamma\right) &= \frac{2F\alpha}{\pi}\left(G_8^s + \frac{2}{3}G_{27}\right) M_K^2 i\varepsilon^{\mu\nu\rho\sigma} k_{1\rho} k_{2\sigma} \\ &\times \left(\frac{1}{M_K^2 - M_\pi^2} + \frac{(c_\theta - 2\sqrt{2}s_\theta)(c_\theta - \sqrt{2}s_\theta)}{3(M_K^2 - M_\eta^2)} + \frac{(s_\theta + 2\sqrt{2}c_\theta)(s_\theta + \sqrt{2}c_\theta)}{3(M_K^2 - M_{\eta'}^2)}\right), \end{aligned} \tag{12}$$

turns out to be dominated by the η:

$$\mathcal{A}^{\mu\nu}\left(K_L \to \gamma\gamma\right) = \left(G_8^s + \frac{2}{3}G_{27}\right)\left[(0.46)_\pi - (1.83 \pm 0.30)_\eta - (0.12 \pm 0.02)_{\eta'}\right] i\varepsilon^{\mu\nu\rho\sigma} k_{1\rho} k_{2\sigma}, \tag{13}$$

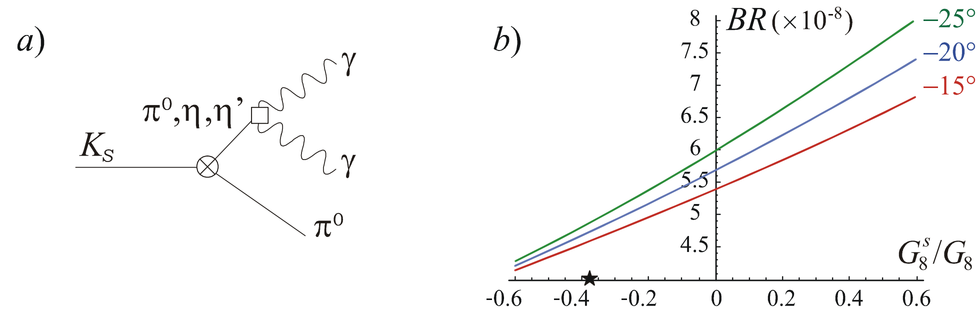

Figure 2: a) Pole diagrams for $K_S \to \pi^0\gamma\gamma$. b) $\mathcal{B}\left(K_S \to \pi^0\gamma\gamma\right)$ as a function of G_8^s/G_8 for $\theta_P = -15°, -20°, -25°$. The star refers to the theoretical value given in Eq.(14).

and is quite stable with respect to the η_8-η_0 mixing angle θ_P, allowed to vary in the large range $[-25°, -15°]$ to get a hold on the typical size of NLO effects. From the experimental $K_L \to \gamma\gamma$ branching ratio[4], we obtain $(G_8^s/G_8)_{ph} \simeq \pm 1/3$, in agreement with the QCD-inspired value[1]

$$(G_8^s/G_8)_{th} = -0.38 \pm 0.12, \tag{14}$$

leading to $(\mathcal{F}_P)_{th} \simeq 60\%$.

4 $K_S \to \pi^0\gamma\gamma$ - the simplest probe

The simplest mode to test $(G_8^s/G_8)_{th+ph} \simeq -1/3$ is $K_S \to \pi^0\gamma\gamma$. Indeed, at leading order in the chiral expansion, i.e., $\mathcal{O}(p^4)$, it proceeds entirely through pole diagrams (Fig.2a). It receives contributions from $\hat{Q}_1$ and $\hat{Q}_6$, but not $\hat{Q}_2$, or correlated contributions from Q_8^s, Q_{27} and Q_8 in the natural $U(3)$ basis. The latter dominates the decay via the pion pole. When η_0 effects are integrated out, the standard $SU(3)$ result[5] is recovered:

$$\mathcal{B}\left(K_S \to \pi^0\gamma\gamma\right)^{SU(3),\mathcal{O}(p^4)}_{m_{\gamma\gamma}>220\text{ MeV}} = 3.8 \times 10^{-8}\;. \tag{15}$$

However, the contribution of the η_0 meson, despite non-leading, can significantly enhance the branching fraction (Fig.2b). For our preferred value (14) and $\theta_P \in [-25°, -15°]$, we obtain:

$$\mathcal{B}\left(K_S \to \pi^0\gamma\gamma\right)^{U(3),\mathcal{O}(p^4)}_{m_{\gamma\gamma}>220\text{ MeV}} = (4.8 \pm 0.5) \times 10^{-8}\;, \tag{16}$$

where the theoretical error only reflects the ranges assigned to G_8^s/G_8 and θ_P. The current experimental value is[6]:

$$\mathcal{B}\left(K_S \to \pi^0\gamma\gamma\right)^{\exp}_{m_{\gamma\gamma}>220\text{ MeV}} = (4.9 \pm 1.8) \times 10^{-8}\;. \tag{17}$$

Note that a more precise measurement could already fix the sign of G_8^s/G_8.

5 $K^+ \to \pi^+\gamma\gamma$ - a promising probe

The case of $K^+ \to \pi^+\gamma\gamma$ is slightly more involved as it proceeds through both loop and pole diagrams at leading order in the chiral expansion, i.e., again, $\mathcal{O}(p^4)$. Still, these two types of contributions correspond to photons in different CP eigenstates, and do not interfere in the rate. The usual $SU(3)$ analysis, including unitarity corrections, can thus be applied to the loops while the poles (Fig.3a), sensitive to η_0 effects, are better treated within the $U(3)$ framework.

Unlike for $K_S \to \pi^0\gamma\gamma$, the pion pole contribution from Q_8 plays a minor role here as $K^+ \to \pi^+\pi^0$ is purely $\Delta I = 3/2$ when on-shell. The pole amplitude is thus quite sensitive to

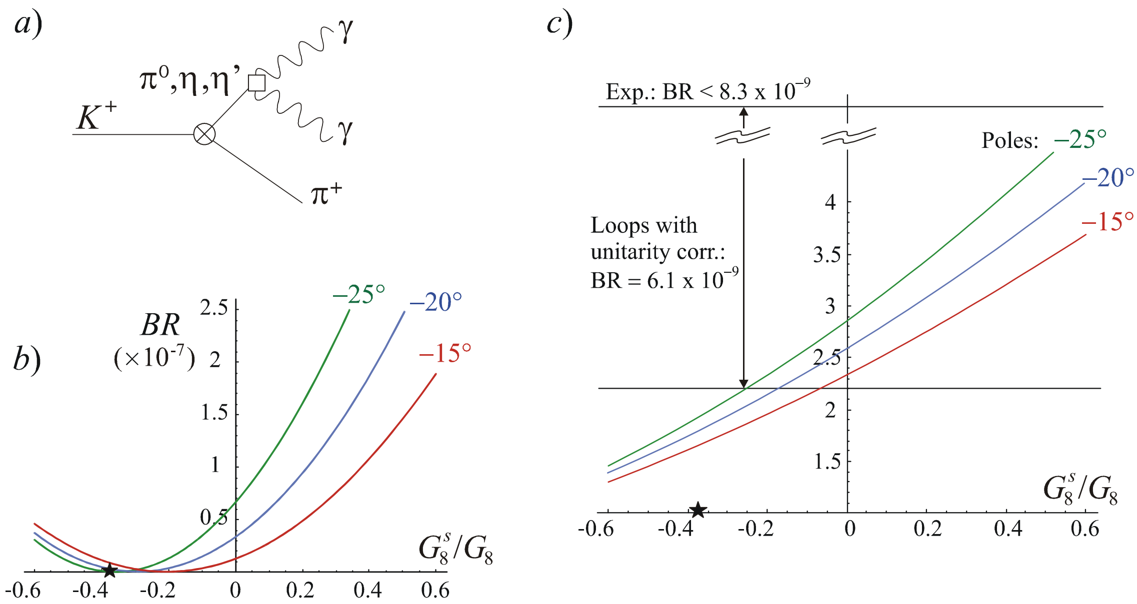

Figure 3: a) Pole diagrams for $K^+ \to \pi^+\gamma\gamma$. b) $\mathcal{B}\left(K^+ \to \pi^+\gamma\gamma\right)^{poles}$ as a function of G_8^s/G_8 for $\theta_P = -15°, -20°, -25°$. c) $\mathcal{B}\left(K^+ \to \pi^+\gamma\gamma\right)^{poles}$ for $m_{\gamma\gamma} < 108$ MeV, $\times 10^9$. Assuming non-negligible loop contributions[8], the recent upper bound[10] hints towards negative values for G_8^s/G_8. The stars refer to Eq.(14).

Q_8^s and Q_{27}. Already at the $SU(3)$ level, when η_0 effects are discarded, one can see that the 27 operator actually accounts for about half of the pole-induced branching fraction:

$$\mathcal{B}\left(K^+ \to \pi^+\gamma\gamma\right)^{\mathrm{P},SU(3),\mathcal{O}(p^4)}_{m_{\gamma\gamma}>220\text{ MeV}} = 1.17 \times 10^{-7}\ , \tag{18}$$

instead of 0.51×10^{-7} without Q_{27}[7]. The contribution of the η_0 meson may substantially suppress or enhance this value, depending on G_8^s/G_8 (Fig.3b).

In particular, for $G_8^s/G_8 = -0.38\pm0.12$ and $\theta_P \in [-25°, -15°]$, poles can be safely neglected with respect to loops:

$$\mathcal{B}\left(K^+ \to \pi^+\gamma\gamma\right)^{\mathrm{P},U(3),\mathcal{O}(p^4)}_{m_{\gamma\gamma}>220\text{ MeV}} \lesssim 0.3 \times 10^{-7}\ , \tag{19}$$

while, for $G_8^s/G_8 > 0$, they could increase the total rate by more than 20%. In that case, they should be taken into account in the extraction of the $\mathcal{O}(p^4)$ combination of counterterms $\hat{c}$ to reach consistency between the total and differential rates[7,8,9].

Finally, restricting the analysis to the low energy end of the $\gamma\gamma$ spectrum, negative values of G_8^s/G_8 are already favoured (cf. Fig3c).

6 Implication for ΔM_K

Pole diagrams also play a central role in the long distance contribution to the K_L-K_S mass difference ΔM_K (Fig.4a). The situation here is quite similar to the one of $K_L \to \gamma\gamma$, in that the contribution of Q_8 vanishes both in $SU(3)$ and $U(3)$ ChPT at $\mathcal{O}(p^4)$, the leading effect being driven by the $\hat{Q}_1$ operator, i.e., a $u\bar{u}$ pair (Fig.4b). The resulting pole formula was worked out in our original paper[1]. Its contribution to ΔM_K is summarized in Fig.4c. For the preferred value Eq.(14), the negative contribution of poles partially cancels the positive contribution of $\pi\pi$ loops, leaving to short-distance effects[11] the task of reproducing the bulk of the observed mass difference.

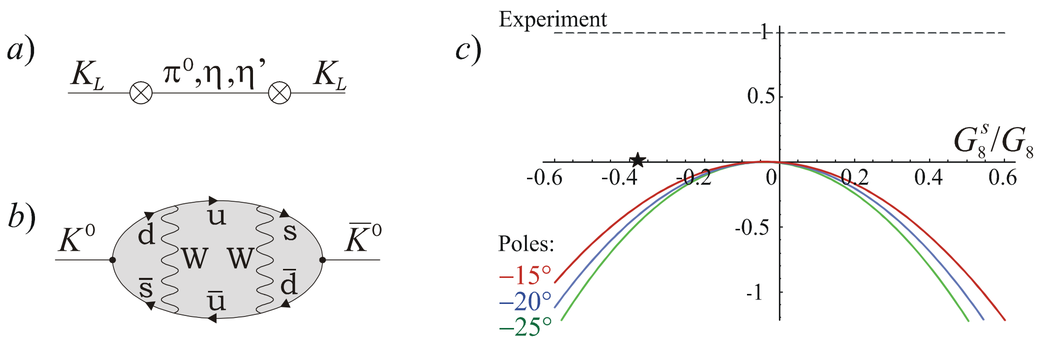

Figure 4: a) Pole diagrams for ΔM_K^{LD}. b) Long-distance $\bar{u}u$ contribution. c) Fraction of pole contribution to ΔM_K^{exp} as a function of G_8^s/G_8 for $\theta_P = -15°, -20°, -25°$. The star refers to Eq.(14).

7 Conclusion

The $\Delta S = 1$ effective operator Q_8^s, which describes pure η_0 effects, holds the key to a phenomenological extraction of the penguin fraction in $K \to \pi\pi$ amplitudes via the change of chiral basis $(\hat{Q}_1, \hat{Q}_2, \hat{Q}_6) \leftrightarrow (Q_8, Q_{27}, Q_8^s)$.

From $\mathcal{B}(K_L \to \gamma\gamma)$, we found $G_8^s/G_8 \simeq -1/3$, which corresponds to a rather smooth non-perturbative current-current operator evolution and a penguin contribution to the $\Delta I = 1/2$ rule around 2/3 at the hadronic scale. Better measurements of the decays $K_S \to \pi^0\gamma\gamma$ and $K^+ \to \pi^+\gamma\gamma$ would provide important tests of this picture.

The recourse to (broken) $U(3)$ chiral symmetry also allowed us to identify correctly the leading contribution to $K_L \to \gamma\gamma$, namely the transition $K_L \to u\bar{u}$ generated by $\hat{Q}_1$. This results in a new pole formula, based on $\hat{Q}_1$ instead of $\hat{Q}_6$. For $G_8^s/G_8 < 0$, the sign of the interference between the short-distance and dispersive $\gamma\gamma$ amplitudes in $K_L \to \mu^+\mu^-$ is flipped.

Along the same lines, the pole contribution to ΔM_K^{LD} was shown to be essentially due to $\hat{Q}_1$, pleading again for a better knowledge of the low-energy constants x_i, that is to say, of G_8^s.

Acknowledgments: S.T. would like to thank the organizers of the XLIrst Rencontres de Moriond. J.-M.G. acknowledges support by the Belgian Federal Office for Scientific, Technical and Cultural Affairs through IAP P5/27; C.S. is supported by the Schweizerischer Nationalfonds; S.T. is supported by the DFG grant No. NI 1105/1-1; this work has also been supported in part by IHP-RTN, EC contract No. HPRN-CT-2002-00311 (EURIDICE).

References

1. J.-M. Gérard, C. Smith and S. Trine, Nucl. Phys. **B730** (2005) 1.
2. http://na48.web.cern.ch/NA48/NA48-2/Overview/results.html.
3. W. A. Bardeen, A. J. Buras and J.-M. Gérard, Phys. Lett. **B180** (1986) 133; Nucl. Phys. **B293** (1987) 787; Phys. Lett. **B192** (1987) 138.
4. A. Lai *et al.* [NA48 Collaboration], Phys. Lett. **B551** (2003) 7. M. Adinolfi *et al.* [KLOE Collaboration], Phys. Lett. **B566** (2003) 61.
5. G. Ecker, A. Pich and E. de Rafael, Phys. Lett. **B189** (1987) 363.
6. A. Lai *et al.* [NA48 Collaboration], Phys. Lett. **B578** (2004) 276.
7. G. Ecker, A. Pich and E. de Rafael, Nucl. Phys. **B303** (1988) 665.
8. G. D'Ambrosio and J. Portolés, Phys. Lett. **B386** (1996) 403; err. *ibid.*, **B389** (1996) 770.
9. P. Kitching *et al.* [E787 Collaboration], Phys. Rev. Lett. **79** (1997) 4079.
10. A. V. Artamonov *et al.* [E949 Collaboration], Phys. Lett. **B623** (2005) 192.
11. S. Herrlich and U. Nierste, Nucl. Phys. **B419** (1994) 292.